SPEKTRA: Jurnal Fisika dan Aplikasinya
Volume 10, Issue 1, April 2025
Homepage: doi.org/10.21009/SPEKTRA

DOI: doi.org/10.21009/SPEKTRA.101.01

Influence of Polymer Matrix on The Morphology and Crystallization Behavior of Electrospun Zinc Oxide Fibers

Annisa Aprilia[1,*], Diki Permana[2], Lusi Safriani[1], Fitrilawati[1]

[1]*Physics Department, Faculty of Mathematics and Natural Sciences, Universitas Padjajaran, Jl. Raya Bandung-Sumedang KM21, Kabupaten Sumedang, 45633, West Java, Indonesia*
[2]*Bachelor of Physics Study Program, Faculty of Mathematics and Natural Sciences, Universitas Padjajaran, Jl. Raya Bandung-Sumedang KM21, Kabupaten Sumedang, 45633, West Java, Indonesia*

*Corresponding Author Email: a.aprilia@phys.unpad.ac.id

Received: 14 November 2024
Revised: 12 December 2024
Accepted: 30 December 2024
Online: 11 February 2025
Published: 30 April 2025

SPEKTRA: Jurnal Fisika dan Aplikasinya
p-ISSN: 2541-3384
e-ISSN: 2541-3392

ABSTRACT

ZnO finds widespread applications such as in photocatalysis, sensors, medicine, and other optoelectronic devices. The characteristics of ZnO can be influenced by several parameters, one of which is morphology. Fiber structures are attractive for research among various shapes and sizes due to their large effective surface area. ZnO fibers can be produced using electrospinning. However, the fiber morphology strongly depends on several important parameters, one of them is the characteristics of the polymer as a matrix. The molecular weight and concentration of the polymer and precursor material influence the solution viscosity, which is one of the crucial parameters in the electrospinning method. In this study, ZnO fibers were fabricated using three different polymers as matrices: PVP (polyvinyl pyrrolidone), PVAc (polyvinyl acetate), and PVA (polyvinyl alcohol). This research investigates the influence of polymer type on the morphology of ZnO fibers and crystallization behavior based on thermal characteristics. Based on SEM results, ZnO fibers were successfully fabricated with diameters ranging from 20–90 nm. The different characteristics are related to the type of polymer matrices and heating treatment. Only the PVA polymer could produce fibers before and after calcination, whereas the PVAc polymer-based fiber vanished after calcination. The disappearance of the fiber morphology is probably caused by the relatively high precursor (ZnAc) concentration, which leads to damage to the fibers formed during the calcination process. PVP failed to produce fibers, possibly due to its low polymer molecular weight, necessitating adjustment of other

parameters. The removal of organic compounds through calcination continued until a temperature of 450ºC was reached. However, organic compounds were still identified in the samples based on FTIR characteristics. The ZnO/PVA fibers have hydrophobic surfaces, with the contact angle of water droplets being 117.75º. This characteristic is ideal for several applications such as antibacterial compounds or self-cleaning materials. Considering the inherent properties of ZnO, it can function as both an antibacterial and a photocatalytic agents simultaneously.

Keywords: ZnO fiber, electrospinning, polymer matrix, sol-gel, TGA-DTA

INTRODUCTION

One of the materials currently being extensively developed is semiconductor material-based metal oxides. Among the types of metal oxides, zinc oxide (ZnO) is a functional material because of its superior properties and suitability for several technological applications. It offers relatively simple processes, inexpensive production, and an environment-friendly nature [1]. ZnO has a direct wide bandgap energy of 3.37 eV, located in the near-UV spectral region, with strong oxidation ability, good photocatalytic properties, and a large exciton binding energy at room temperature of 60 meV [2]. As a result, the exciton emission process can be sustained at room temperature or even above [3]. These metal oxides is widely applied in various applications such as gas sensors, biochemical sensors, photonic crystals, photodetectors, photodiodes, light-emitting devices, transistors, photovoltaics or solar cells, antibacterial agents, and photocatalysts [4, 5].

ZnO with particular structures in lower dimensions (0, 1, and 2 dimensions) has been reported to exhibit better performance in practical applications. The morphology and sizes of various structures are currently being extensively developed and used as needed in the development of applications. Based on many reports, ZnO can be formed into various nano-morphologies such as nanocrystals, nanofibers, nanorods, nanodiscs, nanowires, nanosheets, and nanotubes. These nano-morphologies have been used for practical purposes. Nanofibers have gained much attention among the various types and forms of nanostructures [6]. ZnO nanofibers offer a highly effective surface area and possess suitable optoelectronic properties. This condition makes ZnO nanofibers highly suitable for photocatalytic, photovoltaic, DSSC, and gas sensor applications [7, 8]. Due to the highly effective surface area, the fiber structure provides a defined low pattern along the longer dimension, contributing to increased photocatalytic efficiency [9]. The morphology of ZnO nanostructures, especially one-dimensional forms, can enhance the performance of perovskite solar cells by boosting electron mobility and minimizing charge carrier losses [10]. Moreover, the morphology of materials in gas-sensing devices impacts sensing performance related to surface chemical reactions and gas diffusion. The larger pore size and the higher porosity are more favorable in gas diffusion [8]. ZnO nanograins immobilized on the polymer matrix have been reported to create a metallic volume at the boundaries, enhancing the sensitivity and selectivity of H_2 gas [11].

The ZnO in fiber forms can be produced using the electrospinning technique. Electrospinning is a simple technique commonly used to produce nanofibers with diameters ranging from 10–100 nm [7]. Electrospinning is an excellent method to create various types of fibers, such as polymer, composite, organic, and ceramic fibers, with high surface-to-volume ratios and uniform diameters ranging from nanometers to micrometers [12]. Although electrospinning is a simple technique, several important parameters significantly affect the quality, morphology, and structure of the resulting nanofibers, and these parameters need to be well-considered. One of the key electrospinning parameters relates to the precursor solution as a main raw material. The physical parameters of the precursor solution are conductivity, concentration, viscosity, surface tension, and molecular weight. These physical parameters play an important role and must be considered and adjusted in relation to the other parameters in the electrospinning apparatus [13]. The parameters that relate to the electrospinning apparatus include applied voltage (V), the distance from the needle tip to the collector (d_t), collector shape, needle diameter, and feed rate (v). These apparatus parameters are illustrated in FIGURE 1. The choice of the apparatus parameters needs to be adjusted to match the precursor solution's physical parameters. For example, the highest conductivity of raw solution needs a lower applied voltage, or even a lower viscosity needs a short needle tip distance ($<d_t$). Ambient conditions such as humidity and environmental temperature are also important considerations in electrospinning. Although the fiber's surface and morphology characteristics depend on the application, having small pore sizes and large surface areas has recently become the dominant required characteristic [14].

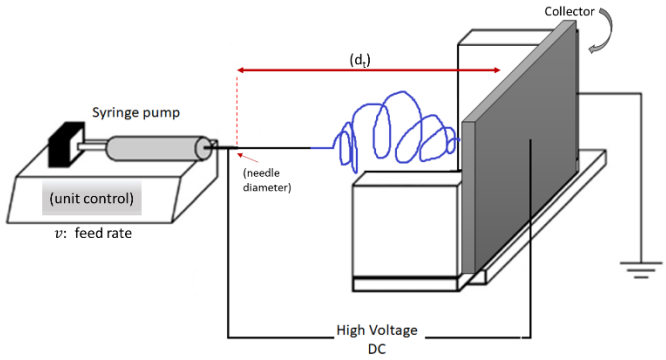

FIGURE 1. Schematic of electrospinning apparatus with its parameters.

It is difficult to adjust all parameters to produce the desired morphology (small pore sizes and large surface areas) of ZnO fibers via electrospinning. One crucial parameter is the choice of polymer as a matrix to immobilize the ZnO particles. Polymer concentration and polymer molecular weight are related to the type of polymer used. The molecular weight indicates the length of a polymer chain, where longer polymer chains correspond to higher molecular weights. Solution precursor viscosity strongly correlates with the type of polymers, material concentration, and solvent. In research conducted by Kim & Lee (2008), ZnO nanofibers 150 – 580 nm in diameter were successfully prepared using polyvinyl alcohol (PVA) with a polymer molecular weight of 85×10^3 – 124×10^3 g/mol [15]. Guo et al. (2013) also successfully produced ZnO fibers with diameters between 90 and 150 nm using polyvinyl

pyrrolidone (PVP) with a molecular weight of 1.6×10^6 g/mol [16]. Meanwhile, in another study by Kim et al. (2007), polyvinyl acetate (PVAc) with a molecular weight of 10×10^{-6} g/mol was used to produce ZnO nanofibers with diameters of 200 – 500 nm, which were applied as photoanodes in DSSC materials [17]. The molecular weight affects the viscosity of a solution, with the viscosity of a polymer solution being directly proportional to the mass of the polymer and its molecular weight [18].

The electrospinning method is quite challenging due to the numerous parameters that must be considered. Several studies using the same set of parameters have reported different fiber outcomes. Therefore, this study emphasizes how ZnO fibers are produced using the same equipment and precursor but with different polymers. Thermal stability is closely related to the type of polymer used. Differences in precursor concentration for the same kind of polymer can affect the thermal properties due to chemical reactions between the two compounds. The use of three common polymers as a matrix was studied based on previous results reported by other researchers. The three polymers are PVP (polyvinyl pyrrolidone), PVAc (polyvinyl acetate), and PVA (polyvinyl alcohol). Zinc acetate dihydrate is used as a precursor for the ZnO raw material. This study investigates how a different polymer types can produce different fiber characteristic. The correlation between crystallization properties during heating treatment and the resulting fiber structure and morphology is discussed. The viscosity of all solution precursors was adjusted in relation to the polymer characteristics, such as solving solution, molecular weight, and boiling point.

METHOD

The ZnO fibers were made in several steps using an electrospinning apparatus (up to 20 kV). The first step involved preparing a precursor solution using Zn(CH3COOH)2—2H2O (ZnAc) with Dimethylformamide (DMF) and deionized water (DI) as solvents. DMF was used as a solvent for PVP and PVAc, while DI was used as the solvent for PVA. The physical characteristics of the polymers, concentration of all materials, and electrospinning parameters used in these experiments are tabulated in TABLE 1.

TABLE 1. Physical properties of precursor solution and parameter settings of electrospinning.

Polymer	(M_w) x 10^3g/mol	Boiling Point ◦C	Viscosity (mPas)	Polymer: ZnAcetate	V (volt)	*v* (mL/h)	T(◦C)	d_t (cm)
PVP	4.0	217.6	104	1 : 1	12 k	0.5	450	9
PVA	47.3	340	198	2 : 1	15 k	0.3	500	9
PVAc	500	150	78	2 : 1	18 k	0.3	450	9

The precursor solution is placed into a 1 mL syringe with a 23G needle. The filled syringe is connected to the syringe pump of the electrospinning apparatus, where the distance from the needle tip to the collector plate is set to 9 cm. The collector plate is covered by aluminum foil, and the ITO glass substrate is attached to the aluminum foil-covered collector plate. The ITO substrate is aligned with the needle. Depending on the polymer type, the applied voltage ranges

between 12 and 18 kV. The syringe flow rate is set to 0.3 to 0.5 mL/hour. ZnAc/polymer fibers are successfully deposited on the ITO substrate, forming a homogeneous white layer on the collector. The samples are calcinated to remove the polymer (organic compounds) from the resulting fibers and convert them into ZnO crystal fibers. The calcination process is conducted using a hot plate at 90 °C for 10 minutes. The temperature is then increased by 15 °C every 3 minutes until it reached 450° to 500 °C for 1 hour for ZnO crystallization. All prepared samples are characterized using Scanning Electron Microscopy (SEM) JEOL JSM-6510 LA to observe the fiber morphology. The ZnO crystal structure is analyzed using X-ray diffraction (XRD). The existence of organic compounds and other functional groups is identified using Fourier Transform Infrared Spectroscopy (FTIR). The thermal properties are characterized using Thermogravimetric-Differential Thermal Analysis (TG/DTA). Contact angle measurements are conducted to determine the wettability characteristic of the fiber surfaces.

RESULTS AND DISCUSSION

The differences in parameters related to polymers, such as ZnAc concentration and solution viscosity, are noteworthy. Zinc acetate dihydrate serves as the raw material for ZnO, and the original fiber consists of organic compounds derived from polymers and precursors. Calcination at specific temperature is necessary to obtain pure ZnO fibers, remove organic compounds, and facilitate ZnO crystallization. FIGURE 2 displays photographs of the fiber layers before and after calcination for all samples. In FIGURE 2(a), the ZnAc/PVP sample appears colorless and transparent. After calcination, the ITO glass substrate turns white while maintaining a thin layer. FIGURE 2(c) and (d) illustrate the physical appearance of the ZnAc/PVAc (before calcination) and ZnO/PVAc (after calcination) fiber layers. Before calcination, the ZnAc/PVAc sample appears thick, opaque, white, and relatively homogeneous. After calcination, the ZnO/PVAc layer fades and shrinks, as shown in FIGURE 2(d), but remains relatively thicker than the ZnO/PVP sample. FIGURE 2(e) presents the physical appearance of the ZnAc/PVA fiber layer before calcination. This layer appears white, homogeneous, and thick, with a smooth and dry surface texture, which makes peeling off the ITO substrate easy. After calcination (FIGURE 2(f)), the layer's appearance does not significantly differ from the layer's appearance before calcination.

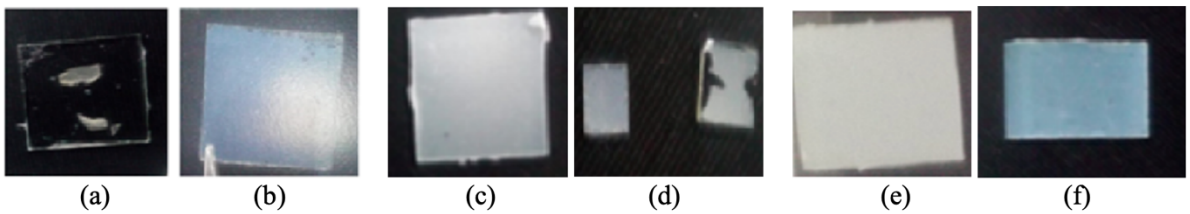

FIGURE 2. The samples photographed before(ZnAc/polymer) and after calcinated (a) ZnAc/PVP, (b) ZnO/PVP, (c) ZnAc/PVAc, (d) ZnO/PVAc, (e) ZnAc/PVA and (f) ZnO/PVA.

Fiber morphology of all samples is investigated using a scanning electron microscope (SEM), as shown in FIGURE 3. The images show all samples before and after calcination. Fiber morphology is observed for the ZnAc/PVAc (FIGURE 3(a)) and ZnAc/PVA (FIGURE 3(b)), while ZnAc/PVP (FIGURE 3(c)) does not show fiber forms. This situation is expected to relate

to the physical parameters of the precursor solution. The viscosity of the ZnAc/PVP precursor solution is 104 mPas, which is sufficient for the electrospinning method [15]. The viscosity of the solution interacts with other electrospinning parameters, such as applied voltage and distance between the nozzle and collector. The molecular weight of the PVP used is 4×10^4 g/mol, which is lower than that reported in other previous studies [17]. The mass ratio of ZnAc and PVP used also needs consideration. In this case, the mass of the polymer compared to the mass of ZnAc is equal (1:1), which means that the acetate concentration inside the solution precursor is high. High acetate concentrations could lead to chain scission or degradation of PVP, which might reduce the molecular weight of the polymer and negatively impact fiber strength and integrity. The presence of acetate could impact the electrical conductivity of the solution, affecting the electrospinning process. Therefore, for PVP, the highest voltage (20 kV) was applied as compensation. As the voltage increases, the electrostatic force generated also increases. However, the magnitude of the electrostatic force during electrospinning must be balanced with the length and strength of the polymer chain bonds in the polymer solution used. Using a high voltage can break polymer chains, preventing fiber formation on the collector. This situation likely occurred in ZnAc/PVP sample (before calcination) or in ZnO/PVP (FIGURE 3(d) after calcination), resulting in no fiber formation.

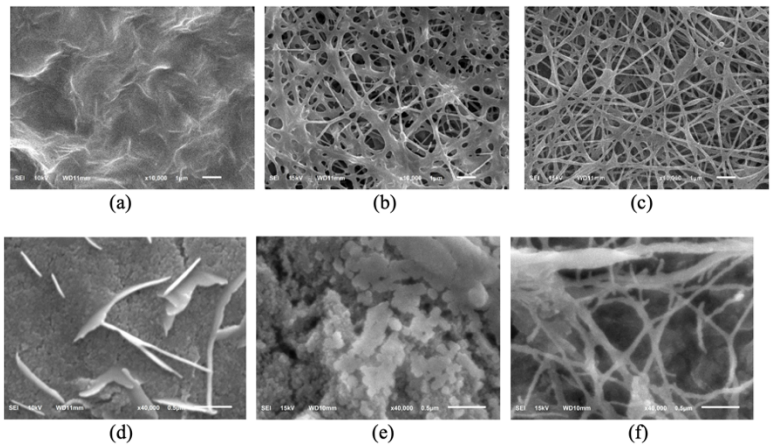

FIGURE 3. SEM images of the samples (a) ZnAc/PVP, (b) ZnAc/PVAc, (c) ZnAc/PVA, (d) ZnO/PVP, (e) ZnO/PVAc, and (f) ZnO/PVA

The fiber morphology of the sample with PVAc before and after calcination is shown in FIGURE 3(b) and 3(e). The fibers formed have an irregular morphology, are less continuous and homogeneous, lack beads, and show overlapping fibers, resulting in significant agglomeration. The relatively high voltage of 18 kV may cause the observed agglomeration. The use of high voltage accelerates the electrospinning process; however, the fibers collected on the collector require time to dry. However, if the fiber emission from the needle occurs too quickly, the fibers will stack and not have enough time to dry, causing the fibers formed to tend to merge. After calcination (FIGURE 3(e)), the fiber morphology disappears and remains the spherical form of ZnO. FIGURE 3(c) shows the ZnAc/PVA sample before calcination, where the sample exhibits the best fiber morphology compared to the others. The fiber form of ZnAc/PVA is a relatively uniform, continuous, homogeneous morphology with minimal

agglomeration. Setting up the right parameters contributes to the production of well-formed fibers. The calcination at 450°C was carried out to produce ZnO fibers, as shown in FIGURE 3(f). The shape of the fiber can still be maintained even though some parts appear damaged.

The ZnO fiber crystal structure is identified using XRD characterization to investigate the successive ZnO fiber preparation. Since the fiber morphology is shown in only two samples (PVAc and PVA), the XRD measurement is conducted only for ZnO/PVAc and ZnO/PVA. FIGURE 4(a) shows the XRD pattern of the two fiber samples and also the crystallography open database (COD) of ITO (indium tin oxide) and ZnO, with the numbers No.1010341 (*Indium oxide*) and No.9008877 (*zincite*). The diffraction peaks of ZnO are marked with black triangle symbols, while those of indium oxide are marked with yellow circle symbols. The peaks of ZnO crystals from both the ZnO/PVAc and ZnO/PVA samples are (100), (002), (101), (012), (110), (013), (112), and (201), confirming that the crystal structure formed is hexagonal wurtzite [19]. Some peaks that do not correspond to either ZnO or the ITO substrate are identified in the ZnO/PVAc sample. Within the 2θ range of 0º to 30º, three unidentified peaks appear at 9º, 19º, and 28º. These peaks are identified as $Zn(AcO)_2$ ($(CH_3CO_2)_2Zn$), which was not decomposed during the calcining process [20]. To investigate further this impurity, FTIR characterization and thermal gravimetry analysis (TGA) of the samples are carried out.

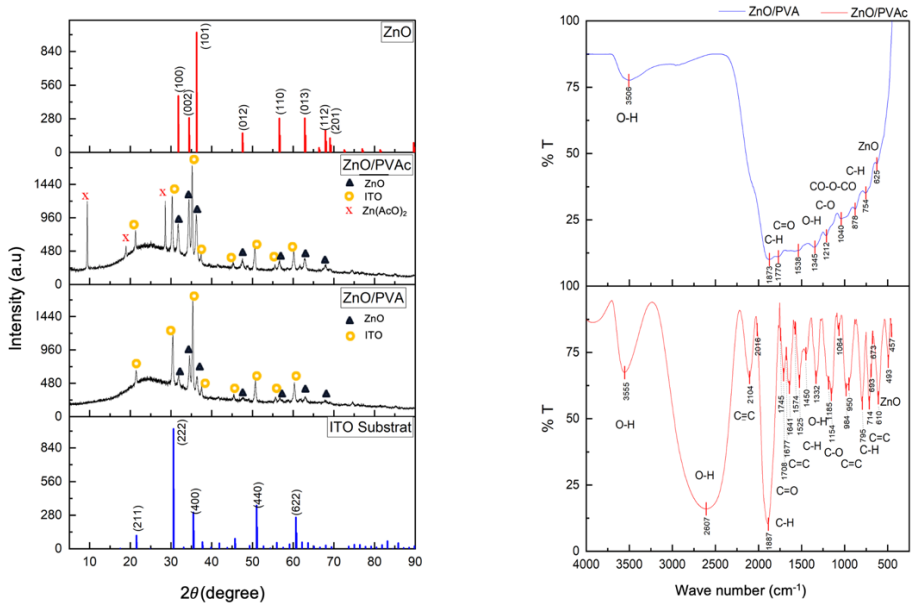

(a) (b)

FIGURE 4. (a). X-ray diffraction pattern of ZnO/PVAc and ZnO/PVA, (b) Fourier Transform infrared spectra of ZnO/PVAc and ZnO/PVA.

FIGURE 4(b) presents the FTIR spectra of ZnO/PVAc and ZnO/PVA, which were conducted to investigate the functional groups. In the ZnO/PVA sample, an absorption peak occurs at a wavenumber of 3506 cm^{-1}, indicating O-H stretching functional groups. Additional absorptions are observed at wavenumbers of 1873 cm^{-1}, 1770 cm^{-1}, 1345 cm^{-1}, 1212 cm^{-1}, 1040 cm^{-1}, and 754 cm^{-1}, corresponding to C-H bending, C=O stretching, O-H bending, CO-

O-CO stretching, and C-H bending, respectively. These organic functional groups, such as O-H, C=O, and C-H, are characteristic of the precursor material and may also originate from the PVA polymer [21]. The absorption at 878 cm^{-1} is attributed to the formation of tetrahedral coordination of ZnO, while the peak at 625 cm^{-1} indicates stretching vibrations from ZnO particles [22]. For the ZnO/PVAc sample (red curve), the absorption peak at 3555 cm^{-1} indicates O-H stretching functional groups. Additionally, O-H stretching is observed at 2607 cm^{-1}, associated with carboxylic acid. The peak at 2104 cm^{-1} results from C≡C stretching. The range from 2000 cm^{-1} to 1000 cm^{-1} includes several functional groups, such as C-H bending, C=O stretching, C=C stretching, O-H bending, and C-O stretching. Meanwhile, the peaks from 1000 cm^{-1} to 450 cm^{-1} correspond to functional groups such as C=C bending, C-H bending, and Zn-O. Zn-O is detected at absorption peaks of 610 cm^{-1}, 493 cm^{-1}, and 457 cm^{-1} [23].

Although ZnO has been crystallized at a calcination temperature of 450ºC, this temperature appears insufficient to decompose some organic compounds. The existence of organic compounds revealed by FTIR is related to the amorphous phase observed in the XRD pattern. An amorphous phase in the samples is estimated to originate from polymers and acetate. This suggests that the amorphous structure originates from organic compounds that have not been fully eliminated after calcination due to suboptimal temperatures. To further support this argument, TGA measurements were conducted for both samples.

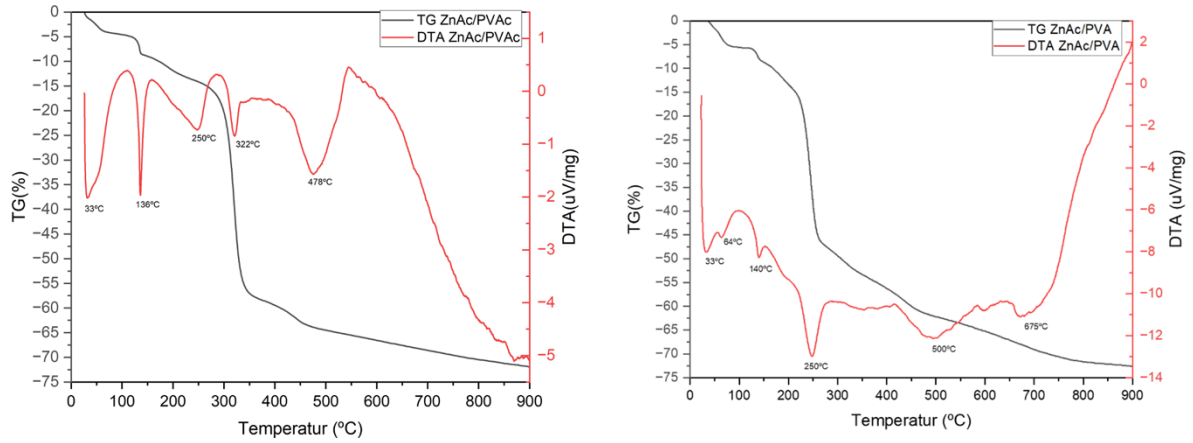

(a) (b)

FIGURE 5. Thermal gravimetry/differential thermal analysis (TGA/DTA) of (a) ZnAc/PVA and (b) ZnAc/PVA.

Based on the TGA results, as shown in FIGURE 5, the suboptimal heating prevented the organic material in the ZnO layer from decomposing completely, leading to residual organic material. In the TGA results, above 450ºC for the ZnO/PVAc sample and 500ºC for the ZnO/PVA sample, endothermic reactions and mass loss still occur, indicating ongoing degradation of organic compounds. These results agree with the FTIR results, where at calcination temperatures of 450ºC for ZnO/PVAc and 500ºC for ZnO/PVA, a significant amount of organic compounds remains, potentially originating from the acetate and polymers. Uncontrolled rapid heating rates during synthesis may also contribute to this situation. Research by Horzum et al. found that Zn(AcO)2 was almost completely decomposed under annealing up to 350°C [24]. The morphology of fiber layers and the existence of polymers as a matrix

seem to influence the thermal characteristics of ZnAcetate. Higher acetate concentrations may lead to more complex decomposition pathways during heating. This can result in variations in thermal stability, such as changes in the temperature at which significant weight loss occurs or the presence of intermediate compounds. To study the thermal properties of the ZnAc/polymers, each endothermic and exothermic reaction is tabulated in TABLE 2.

TABLE 2. Endothermic and exothermic reaction for ZnAc/Polymer identifying the reaction during TGA/DTA measurement.

Thermal reaction	ZnAc/PVAc		ZnAc/PVA		Chemical reaction
	T (°C)	Mass decreases (%)	T (°C)	Mass decreases (%)	
Endothermic	33	5	64	5	Water evaporation started
	136	10	140	8	DMF start to evaporate
	250	25	250	46	Acetate decomposition
	323	60	350	55	Polymer decomposition started
	478	62.5	500	63	ZnO crystallization
Exothermic	100	7.5	100	5	H_2O removing
	170	14	150	10	DMF decomposition
	300	15	280	47	Removing of acetate
	400	60	410	60	ZnO formed
	550	66	675	67	Other organic compound starting to decompose

In a Differential Thermal Analysis (DTA) curve, an endothermic reaction is indicated by a peak pointing downwards, reflecting that the material is undergoing a process that requires energy input, often resulting in changes in its physical or chemical structure [4]. Meanwhile, the exothermic reaction indicates that the material is undergoing a process that releases energy, often resulting in temperature increases and changes in the material's structure. During the thermal analysis of ZnAc/PVAc, the first endothermic reaction occurs at 33ºC. At this stage, the sample begins to absorb heat, leading to the evaporation of water adsorbed on the sample's surface [4, 25]. The next decomposition occurs between 100ºC and 200ºC, where the mass decreases by approximately 5%. The endothermic reaction peak at 136ºC relates to the evaporation of DMF. The mass decreases by about 25% at 250ºC, indicating acetate with some organic materials from PVAc has started to decompose [25, 26]. At the temperature range of 300ºC to 350ºC, ZnO starts to form and crystallize. In this step, the acetate chains break down residual organic material and decompose it. The residual organic material from PVAc is decomposed and removed at 478ºC, and ZnO is fully formed [4, 26]. Meanwhile, from 500ºC to 900ºC, the sample no longer experiences significant mass loss; the reaction occurring is only exothermic at around 550ºC, and after that, the curve continues to decline. This indicates that the organic material may still be in the process of decomposition.

FIGURE 5(b) is the TG/DTA of the ZnAc/PVA sample. Similar to ZnAc/PVAc, at temperatures ranging from 30 ºC to 100 ºC, the sample absorbs heat to initiate the water evaporation. Significant mass loss occurs in the temperature range of 200 ºC to 300 ºC, reducing by approximately 40% and is related to the main reaction of acetate decomposition, the breakdown of some organic materials, and the onset of ZnO crystallisation [15]. A substantial mass reduction continues between 300 ºC and 500 ºC, where the sample mass decreases by about 10%. The research conducted by multiple authors states that ZnO in PVA fibres enhances the decomposition temperature [27, 28]. These results agree with this research that the decomposition temperature of the polymer is estimated to start at ~350 ºC. At 500 ºC, an endothermic reaction indicates the crystallisation of ZnO. This endothermic reaction is due to the decomposition of the organic material residue, a side product of the chemical reaction between raw

materials [15, 29]. A high peak at 675 ºC is estimated to be related to organic material that has not been completely decomposed up to 500 ºC. At a temperature above 800 ºC, the TGA curve tends to be constant, showing a smaller mass reduction.

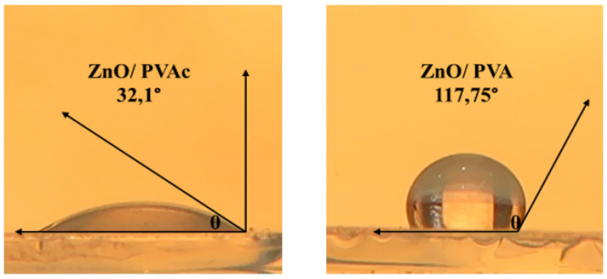

(a) (b)

FIGURE 6. Wettability of the (a) ZnO/PVAc, and (b) ZnO/PVA

The ZnO/PVAc and ZnO/PVA samples were characterised using contact angle measurements to observe surface wettability. The results of the contact angle (CA) measurements for both tested samples are shown in FIGURE 6. The CA of the ZnO/PVAc layer is 32.1º, indicating hydrophilic surfaces. In contrast, the contact angle of the ZnO/PVA sample is 117.75º, which is greater than 90º, indicating that the surface of the ZnO/PVA sample is hydrophobic. The difference in contact angle values between the ZnO/PVAc and ZnO/PVA samples can be attributed to several physical and chemical factors, such as the texture and shape of the sample surfaces, which refer to the degree of roughness and smoothness [30]. Other factors, including the particles' shape and size and the material's surface heterogeneity, can also influence the contact angle [31]. Based on the SEM results, the surface of the ZnO/PVAc sample appears to have a rougher texture with random shapes, sizes, and particle arrangements, facilitating reactions between the surface and the liquid, resulting in a smaller contact angle. In contrast, the surface of the ZnO/PVA sample, as observed in the SEM tests, shows a more regular shape and structure, evidenced by the presence of fibres. Due to surface tension, the structured fibre arrangement hinders the reaction between the liquid and the sample surface, leading to a larger contact angle.

To summarise and understand how a different polymer matrix can produce a different fibre characteristic, all the results provided from this research are tabulated in TABLE 3. The correlation between crystallisation properties during heating treatment and the resulting fibre structure and morphology is established. A higher acetate concentration within the samples increases thermal stability, but it cannot maintain the fibre morphology [21]. The ZnO/PVA has relative morphological stability that can maintain the fiber after calcination.

TABLE 3. Summarise of all characterizations related to the fibre form for all samples.

Polymer Matrix	Morphology	Crystal Structure	Functional Groups	Thermal Characteristics	Surface Properties	Summary
PVP	No fibres	-	-	-	-	Further characterization were not conducted relate to fibre not formed
PVAc	Fibres before calcination	ZnO wurtzite hexagonal structure; amorphous phase originated from polymers; the Zn(AcO)2 crystal is detected	Organic groups still present; with a lot of specific absorption FTIR Spectrum	polymer decomposed started at 323^{o}C;	Hydrophilic	Suitable only before calcination; the calcinated at 450 cannot remove the organic compounds, the concentration of the precursor are need adjustable.
PVA	Suitable fibres (before & after calcination)	ZnO wurtzite hexagonal structure; amorphous phase originated from polymers.	Organic groups still present; with a broad of absorption FTIR Spectrum	polymer decomposed started at 350^{o}C;	Hydrophobic	Suitable produce a fibre form, the calcination up to 500C cannot remove the organic compound and the residue, the calcination steps need to be optimized.

CONCLUSION

ZnO fibers have been successfully prepared through electrospinning using a precursor solution of zinc acetate dihydrate (ZnAc) and PVA as the polymer. The type of polymer significantly influences the formation of ZnO fibers. The polymer that can produce suitable fibers both before and after calcination is PVA, while PVAc generates fibers only before calcination. The dissapearance of fiber morphology in the ZnO/PVAc sample is attributed to the rapid calcination rate, high concentration of ZnAc, and lack of a binder. The PVP matrix does not produce fibers forming before or after calcination, which is estimated to be caused by discrepancies in the electrospinning parameter used. Based on the SEM results, the produced ZnO fibers in the PVA matrix exhibit a less homogeneous morphology and structure, with a spread diameters sizes and not evenly distributed across the substrate surface. The XRD analysis indicates that ZnO fibers have a hexagonal wurtzite crystal structure. The excessively rapid heating rate can affect the structure of the resulting fibers. A gradual and controlled heating process is likely crucial in maintaining the morphology of the produced fibers. Considering the thermal properties of each sample, the fibers produced have not yet decomposed entirely up to 500ºC, indicating that the fibers' residual organic material from the polymer may still be present. Acetate decomposition during heating may leave behind residual organic materials that influence thermal behavior. These residues can lead to changes in thermal stability and decomposition characteristics.

The extended decomposition steps with numerous endothermic and exothermic reaction peaks suggest that a longer calcination time with a constant heating rate is required. The curve that continues to decline indicates that the chemical reactions related to the decomposition of the compounds still occur until the heating reaches a temperature of 900 ºC. This argument is supported by the FTIR spectra for both samples, which show the functional groups of organic compounds are still present in the samples. Additionally, the ZnO/PVAc layer had a contact angle of 32.1º (hydrophilic), while ZnO/PVA has a contact angle of 117.75º (hydrophobic). The differences in contact angle are due to surface texture and particle arrangement; the rougher ZnO/PVAc surface allows for better liquid interaction, whereas the structured

ZnO/PVA fibers increase surface tension, leading to a higher contact angle. The fibers that exhibit hydrophobic surfaces are suitable for use as antibacterial compounds or self-cleaning materials. Given the natural properties of ZnO, it can simultaneously serve as both an antibacterial/self-cleaning and photocatalytic active agent. Recently, the use of antibacterial compounds has become common in industrial applications. This research serves as a foundational study for future developments. Although ZnO fibers were successfully produced, there are challenges regarding scalability and reproducibility. The variation in fiber morphology, such as diameter and surface texture, suggests that further optimization of electrospinning parameters is needed for consistent large-scale production. Additionally, the process's reliance on precise heating rates and polymer concentrations may affect reproducibility in different batches. More research is required to improve scalability and consistency in manufacturing ZnO fibers.

ACKNOWLEDGMENTS

This work was financially supported by an Internal Research Grant from Universitas Padjadjaran through the Riset Kompetensi Dasar Unpad (RKDU) Scheme, under contract No. 1844/UN6.3.1/PT.00/2024, dated March 18, 2024.

REFERENCES

[1] P. Supraja, et al., "A simple and low-cost approach for the synthesis and fabrication of ZnO nanosheet-based nanogenerator for energy harvesting and sensing," *Eng. Res. Express*, vol. 3, p. 035022, 2021, doi: 10.1088/2631-8695/ac184b.

[2] N. D. Dien, et al., "Developing efficient CuO nanoplate/ZnO nanoparticle hybrid photocatalysts for methylene blue degradation under visible light," *RSC Adv.*, vol. 13, p. 24505, 2023, doi: 10.1039/d3ra03791f.

[3] A. D. Mauro, et al., "ZnO for application in photocatalysis: From thin films to nanostructures," *Mater. Sci. Semicond. Process.*, vol. 69, pp. 44–51, 2017, doi: 10.1016/j.mssp.2017.03.029.

[4] R. Raji and K. G. Gopchandran, "ZnO nanostructures with tunable visible luminescence: Effects of kinetics of chemical reduction and annealing," *J. Sci. Adv. Mater. Devices*, vol. 2, no. 1, pp. 51–58, 2017, doi: 10.1016/j.jsamd.2017.02.002.

[5] A. Kołodziejczak-Radzimska and T. Jesionowski, "Zinc oxide—from synthesis to application: A review," *Materials*, vol. 7, pp. 2833–2881, 2014, doi: 10.3390/ma7042833.

[6] S. Bose and D. Sanyal, "Synthesis and characterization of ZnO microfiber by electrospinning technique," *Mater. Today: Proc.*, vol. 5, pp. 9860–9865, 2018, doi: 10.1016/j.matpr.2017.10.178.

[7] A. Zainal, et al., "Characterization of ZnO nanofiber on double-layer dye-sensitized solar cells using direct deposition method," *Periódico Tchê Química*, 2020. ISSN: 2179-0302.

[8] A. Katoch, et al., "Highly sensitive and selective H_2 sensing by ZnO nanofibers and the underlying sensing mechanism," *J. Hazard. Mater.*, vol. 286, pp. 229–235, 2015, doi: 10.1016/j.jhazmat.2014.12.007.

[9] F. Panto`, et al., "Photocatalytic degradation of methylene blue dye by porous zinc oxide nanofibers prepared via electrospinning: When defects become merits," *Appl. Surf. Sci.*, vol. 557, p. 149830, 2021, doi: 10.1016/j.apsusc.2021.149830.

[10] M. Manabeng, et al., "A review of the impact of zinc oxide nanostructure morphology on perovskite solar cell performance," *Processes*, vol. 10, p. 1803, 2022, doi: 10.3390/pr10091803.

[11] R. S. Andre, et al., "Sensitive and selective NH_3 monitoring at room temperature using ZnO ceramic nanofibers decorated with poly(styrene sulfonate)," *Sensors*, vol. 18, p. 1058, 2018, doi: 10.3390/s18041058.
[12] N. Bhardwaj and S. C. Kundu, "Electrospinning: A fascinating fibre fabrication technique," *Biotechnol. Adv.*, vol. 28, no. 3, pp. 325–347, 2010, doi: 10.1016/j.biotechadv.2010.01.004.
[13] R. Abdulhussain, et al., "Electrospun nanofibers: Exploring process parameters, polymer selection, and recent applications in pharmaceuticals and drug delivery," *J. Drug Deliv. Sci. Technol.*, vol. 90, p. 105156, 2023, doi: 10.1016/j.jddst.2023.105156.
[14] A. Al-Abduljabbar and I. Farooq, "Electrospun polymer nanofibers: Processing, properties, and applications," *Polymers*, vol. 15, no. 1, p. 65, 2023, doi: 10.3390/polym15010065.
[15] Y. Kim, et al., "Characterization of electrospun ZnO nanofibers," *J. Korean Phys. Soc.*, vol. 53, pp. 421–425, 2008, doi: 10.3938/jkps.53.421.
[16] G. Yang, et al., "One-dimensional CdS/ZnO core/shell nanofibers via single-spinneret electrospinning: Tunable morphology and efficient photocatalytic hydrogen production," *Nanoscale*, no. 24, 2013, doi: 10.1039/c3nr03462c.
[17] I.-D. Kim, et al., "Dye-sensitized solar cells using network structure of electrospun ZnO nanofiber mats," *Appl. Phys. Lett.*, vol. 91, p. 163109, 2007, doi: 10.1063/1.2799581.
[18] S. Khataei, et al., "Effect of molecular weight and content of polyvinylpyrrolidone on cell proliferation, loading capacity and properties of electrospun green tea essential oil-incorporated polyamide-6/polyvinylpyrrolidone nanofibers," *J. Drug Deliv. Sci. Technol.*, vol. 82, p. 104310, Apr. 2023, doi: 10.1016/j.jddst.2023.104310.
[19] Y. Liao, et al., "Diameter control of ultrathin zinc oxide nanofibers synthesized by electrospinning," *Nanoscale Res. Lett.*, vol. 9, no. 1, p. 267, 2014, doi: 10.1186/1556-276X-9-267.
[20] M. M. Demir, et al., "Precipitation of monodisperse ZnO nanocrystals via acid-catalyzed esterification of zinc acetate," *J. Mater. Chem.*, vol. 16, pp. 2940–2947, 2006, doi: 10.1039/b601451h.
[21] M. Imran, et al., "Fabrication and characterization of zinc oxide nanofibers for renewable energy applications," *Arab. J. Chem.*, vol. 10, pp. S1067–S1072, 2017, doi: 10.1016/j.arabjc.2013.01.013.
[22] N. Jayarambabu, K. V. Rao, and Y. T. Prabhu, "Beneficial role of zinc oxide nanoparticles on green crop production," *Int. J. Multidiscip. Adv. Res. Trends*, vol. 2, no. 1, 2015, doi: 10.1039/C8NJ01849A.
[23] P. Uzalia, et al., "Nanofiber PVA/ZnO sebagai material antimikroba pada wound dressings," *J. Teori dan Aplikasi Fisika*, vol. 11, no. 1, 2023. Available: https://jtaf.fmipa.unila.ac.id/index.php/jtaf/article/view/325.
[24] N. Horzum, M. E. H. Hilal, and T. Isık, "Enhanced bactericidal and photocatalytic activities of ZnO nanostructures changing the cooling route," *New J. Chem.*, no. 14, 2018, doi: 10.1039/C8NJ01849A.
[25] J. H. Kim, et al., "Electrospun ZnO nanofibers as a photoelectrode in dye-sensitized solar cells," *J. Nanoscience Nanotechnol.*, vol. 15, no. 3, pp. 2346–2350, 2015, doi: 10.1166/jnn.2015.10256.
[26] H. Wu and W. Pan, "Preparation of zinc oxide nanofibers by electrospinning," *J. Am. Ceram. Soc.*, vol. 89, no. 2, pp. 699–701, 2006, doi: 10.1111/j.1551-2916.2005.00735.
[27] T. T. Chau, et al., "A review of factors that affect contact angle and implications for flotation practice," *Adv. Colloid Interface Sci.*, vol. 150, no. 2, pp. 106–115, 2009, doi: 10.1016/j.cis.2009.07.003.
[28] K. T. Shalumon, et al., "Sodium alginate/poly(vinyl alcohol)/nano ZnO composite nanofibers for antibacterial wound dressings," *Int. J. Biol. Macromol.*, vol. 49, pp. 247–254, 2011, doi: 10.1016/j.ijbiomac.2011.04.005.
[29] V. H. B. Oliveira, et al., "Electrospun fibers of poly (vinyl alcohol): Zinc acetate (PVA:AcZn) and further ZnO production: Evaluation of PVA:AcZn ratio and annealing temperature effects on ZnO structure," *J. Nanoparticle Res.*, vol. 22, no. 11, 2020, doi: 10.1007/s11051-020-05048-6.

[30] I. Islami, et al., "Low-temperature calcination of TiO_2 and ZnO particle film and evaluation of their photocatalytic activity," *Indones. J. Appl. Phys.*, vol. 13, no. 2, p. 276, 2023, doi: 10.13057/ijap.v13i2.76028.
[31] T. T. Chau, et al., "A review of factors that affect contact angle and implications for flotation practice," *Adv. Colloid Interface Sci.*, vol. 150, no. 2, pp. 106–115, 2009, doi: 10.1016/j.cis.2009.07.003.